Rapid Communications in Mass Spectrometry

WILEY

Rapid Communications in Mass Spectrometry

RESEARCH ARTICLE

Mass Spectrometry Imaging in Archaeobotany: An Illustration Through Analytical Characterisation of Sesame Lignans

Huanxi Li[1,2] | Bin Han[2] | Hongen Jiang[2] | Bo Wang[3] | Mengxuan Chen[4] | Mianbo Ning[4] | Yimin Yang[2]

[1]Key Laboratory of Vertebrate Evolution and Human Origins, Institute of Vertebrate Paleontology and Paleoanthropology, Chinese Academy of Sciences, Beijing, China | [2]Department of Archaeology and Anthropology, School of Humanities, University of Chinese Academy of Sciences, Beijing, China | [3]Xinjiang Uygur Autonomous Region Museum, Urumchi, China | [4]Analytical Applications Center, Shimadzu (China) Co. Ltd., Shanghai, China

Correspondence: Bin Han (bin.han@ucas.ac.cn)

Received: 5 April 2025 | **Revised:** 20 May 2025 | **Accepted:** 20 May 2025

Funding: This study was supported by the Beijing Social Science Foundation Young Academic Leader Project (24DTR077), the National Natural Science Foundation of China (42202211) and the Scientific and Technological Research Projects on Cultural Heritage (2023ZCK008).

Keywords: archaeobotany | MALDI-MSI | pyrolysis | sesame lignans | the Astana Cemetery

ABSTRACT

Rationale: Morphological analysis has been frequently applied in archaeobotany. Recently, increasing studies have been conducted on the identification of biomarkers in archaeobotanical materials, which are rarely attached to morphological analysis. To improve the interpretability of biomarker analysis, the localisation of characteristic biomarkers in ancient samples is needed.

Methods: We analysed characteristic lignans in ancient/modern sesame seeds via matrix-assisted laser desorption ionisation quadrupole time-of-flight mass spectrometry imaging (MSI), testifying the potential of MSI in a detailed discussion of ancient plant use practices.

Results: The MSI distributions of sesamin and sesamolin shared similar traits in modern and ancient sesame seeds while their MSI signals were inhibited by lipidic substances in in situ MSI tests. Besides targeted biomarker characterisation, nontargeted MSI analysis showed potential to reveal plant material treatment process.

Conclusions: Botanical biomarker distribution traits were studied for the first time in archaeobotany. The MSI created a visualised colour plot with localised compound distributions, in which archaeologists can visually aid their study of plant use in antiquity. This, in some cases, provides key information for understanding the livelihoods of ancient people.

1 | Introduction

Archaeobotanical remains encompass both macrobotanical and microbotanical remnants from archaeological sites preserved through various means, such as charring, desiccation or waterlogging, as well as shapeless organic residue [1–3]. The study of plant remains can help in the reconstruction of past environments, climate changes, human activities and social development [4–6]. It can also provide insights into human–plant interactions and interrelationships in the past, including the use of plants and land [7–9], the origin and early development of agriculture [2, 10, 11], and the transformation of livelihoods and social relationships

Huanxi Li and Bin Han contributed equally to this work.

[12, 13]. Typically, studies of plant remains are performed through morphological analysis [2, 3], an easy and effective method that partly and subjectively depends on the researcher's experience and judgment. In some cases, morphological analysis has difficulty identifying poorly preserved archaeological samples, and species present similar morphological traits [14, 15].

The introduction of theories and methods from science and engineering fields has revolutionised archaeobotanical material characterisation and interpretation (especially those of invisible chemical compounds) [2, 16, 17]. This has enhanced our understanding of past plant use. Archaeological biomarkers refer to those compounds that are related to past human activities [18]. In recent decades, with the development of modern analytical techniques, the use of characteristic biomarkers such as cannabis, miliacin and olycyclic aromatic hydrocarbons in archaeobotany and organic residue analysis has played significant roles in revealing the intricacies of ancient ritual, agricultural and technological practices [19–21]. Currently, commonly applied methods for detecting biomarkers include ancient DNA (aDNA) analysis, isotopic studies and gas/liquid chromatography-mass spectrometry (GC-MS/LC-MS) [18].

Mass spectrometry imaging (MSI) is a prominent technology that enables visualisation of the spatial distribution of atoms and molecules in situ [22–24]. It offers precise, label-free detection of a wide range of compounds, requires relatively easy sample preparation methods [22, 23, 25, 26], and has been widely used in various fields, especially in the life sciences, pathology and pharmacology [22, 23, 27, 28]. It serves diverse purposes, including identifying and validating biomarkers related to biotic/abiotic stress [22, 29]. Although only a handful of archaeology studies have used MSI, we can still take a glimpse into the potential of MSI in revealing the use and craft of artefacts. Recently, several archaeological samples have been studied through MSI, such as nondestructive identification of organic dyes in textiles [30], characterisation of lipid preservation in ceramics [31] and determination of the distribution of specific proteins in ancient teeth [32]. Moreover, in the field of cultural heritage preservation, MSI has been conducted on several paintings over the past two decades, providing insights that are not accessible for either morphological or composition analysis [33–35]. These studies either offered alternative ways to determine the presence of certain compounds or helped to optimise the sampling strategies, in which MSI could have implications for revealing more hidden information from archaeological findings.

Sesame (*Sesamum indicum* L., Pedaliaceae) is one of the oldest cultivated plants in antiquity [36]. Sesame contains several lignans, including sesamin, sesamolin and sesamol, with molecular formulas of $C_{20}H_{18}O_6$, $C_{20}H_{18}O_7$ and $C_7H_6O_3$, respectively [37–39]. These compounds are phenolic compounds, a group of natural metabolites known for their ability to retard oxidative stress [40]. In archaeobotany, they can help to identify the use of sesame in archaeological samples [41]. China has a long history of sesame use [41–43]. Some historians believe that Zhang Qian (张骞) first introduced sesame into China during the Western Han Dynasty (202 BC–8 AD) through the Silk Road [43, 44]. Nevertheless, the origin of sesame in China remains controversial [41, 45]. Furthermore, although there are many ancient textual records on sesame that provide us with how ancient humans used sesame, the textual materials are not comprehensive and lack details [41, 45]. Therefore, the study of ancient sesame residues can help clarify the ambiguities in textual materials and provide an unparalleled glimpse into the use of sesame in antiquity.

Xinjiang, a region in northwest China, is characterised by minimal precipitation and high evaporation rates, which results in the prevalent desiccation of archaeological samples, especially well-preserved organic materials [46–49]. It is also a region highlighted for its strategic role in the history of trans-Eurasian migration, cultural communication and crop exchange [50–53]. Archaeological findings in Xinjiang have significantly contributed to our understanding of the complex interactions of ancient people with different cultural backgrounds, available resources and environments [49, 54, 55]. Sesame seeds are sometimes found at archaeological sites in Xinjiang, such as Astana Cemetery, and studies have been carried out to determine how sesame is used and spread [41, 43]. Nevertheless, the distribution of characteristic sesame biomarkers in sesame has not been revealed.

Although MSI analysis has been extensively practiced in the life sciences, it has rarely been applied in archaeobotanical studies. Recent studies have illustrated the effectiveness of biomarker strategies in revealing ancient diets and subsistence strategies [9, 56–58] and encouraged us to develop advanced analytical methods and workflows in archaeobotanical studies [59]. Thus, this work was carried out at a historical site, Astana cemetery, in the Turpan region of Xinjiang. Sesame seeds unearthed from this site were analysed via matrix-assisted laser desorption ionisation mass spectrometry imaging (MALDI-MSI) with the aim of (i) optimising the MALDI-MSI conditions for sesame seed mass spectrometry imaging; (ii) examining the spatial distribution of sesame characteristic lignans (sesamol, sesamin and sesamolin) not obtained via other mass spectrometry techniques; (iii) scrutinising the power of MSI to find evidence of past plant use; and (iv) cultivating the efficiency of MSI for rapid screening of ancient food consumption with easy and visualised data treatment workflows. This study, for the first time, illustrates the efficiency of MSI in archaeobotany studies, revealing an improved characterisation profile and rapid data treatment workflow that contributes to our understanding of plant use, diets and economic activities in antiquity.

2 | Materials and Methods

2.1 | Archaeological Background

The Astana Cemetery is an ancient public graveyard (period of use: 3rd century AD–9th centuries AD) located in Xinjiang Province and contains more than 1000 tombs. This site is 37 km southeast of Turpan city and 6 km north of the ancient city Gaochang (Figure 1). The weather in the area has been extremely arid. Since 1959, Chinese archaeologists have excavated more than 500 tombs. Various objects, such as natural mummies, paper manuscripts, plant and food remnants and textiles,

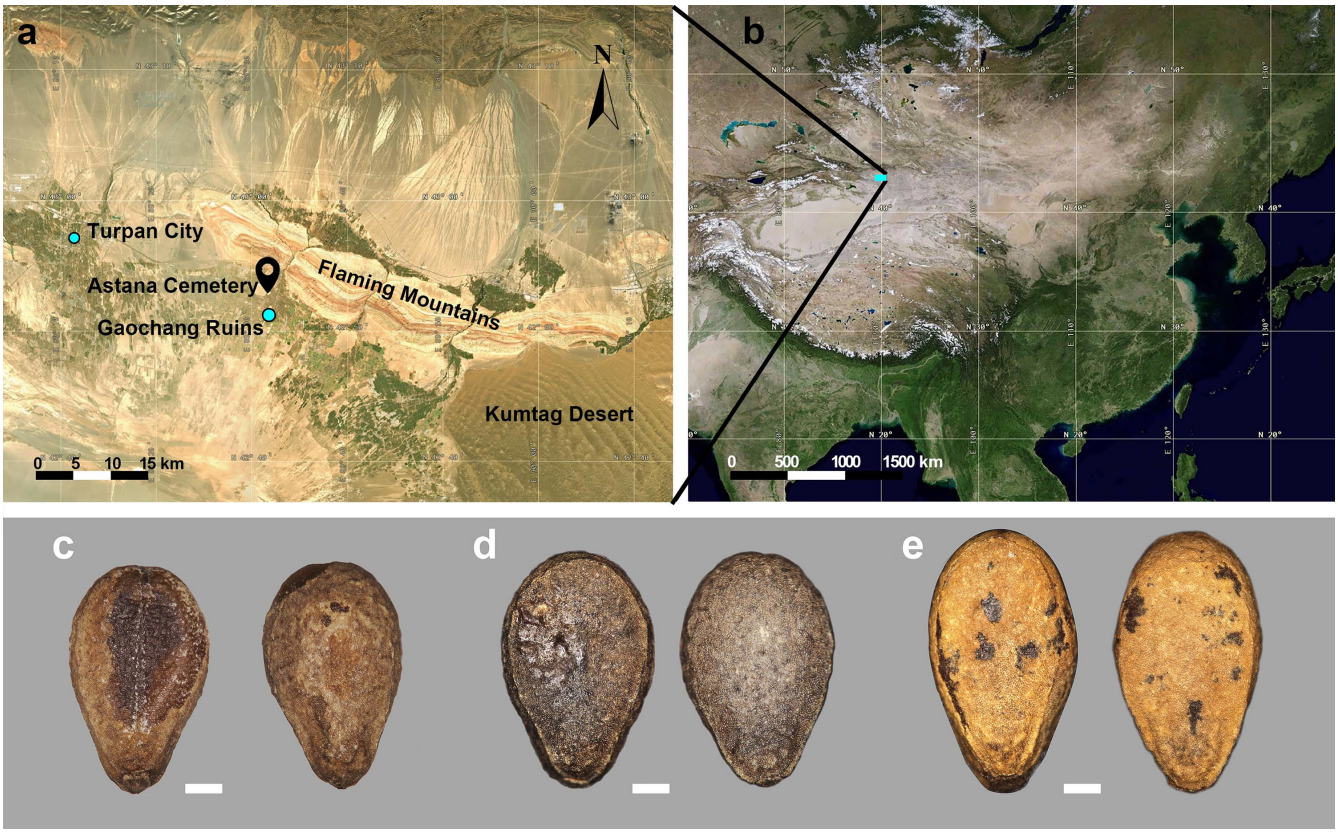

FIGURE 1 | Maps showing the location of the Astana Cemetery and the tested samples. (a) Enhanced satellite view of Astana Cemetery. (b) Astana cemetery in Northwest China. The base maps were from tianditu (https://www.tianditu.gov.cn/), Map Inspection Number: GS (2024) 0568. (c) Sesame seed of AN01. (d) Sesame seed of AN02. (e) Sesame seed of AN03. 1 bar = 500 μm.

have been found and are mostly collected in museums [60]. The earliest macrofossil evidence of sesame use in China, which dates back to approximately the 7th century, was also excavated in the Turpan region [41].

2.2 | Chemicals and Materials

The ancient sesame seeds (AN01, artefact number 72TAM201:34; for AN02 & AN03, the artefact number was unclear; Figure 1c–e) were unearthed from Astana Cemetery. Chen et al. previously identified these samples as sesame seeds through plant macrofossil analysis and pyrolysis analysis [41]. All three samples were dated to the Tang Dynasty (618–907 AD) on the basis of radiocarbon dating data [41]. Reference samples of modern sesame seeds (MBs referred to as roasted, MUs referred to as unroasted) were obtained from a local market.

The sesamin (98%) used in this study was purchased from Macklin Inc., whereas sesamol (95%–99%) and sesamolin (95%–99%) were purchased from ChemFaces Inc. LC/MS grade methanol and dichloromethane were obtained from Merck. Gelatin was obtained from Becton, Dickinson and Company. 2,5-Dihydroxybenzoic acid (DHB), 9-aminoacridine (9AA), neosperidin dihydrochalcone (NEDC), alpha-cyano-4-hydroxycinnamic acid (CHCA), dihydroxyacetone phosphate (DHAP), trans-2-[3-(4-tert-butylphenyl)-2-methyl-2-propenylidene]malononitrile (DCTB), dibemethine (DI) and 1,5-naphthalenediamine (1,5-DAN) were purchased from Sigma-Aldrich.

2.3 | MALDI-MSI Analysis

2.3.1 | Sample Preparation

The samples were first encapsulated within gelatin hydrogels and then placed in a −80°C refrigerator for 0.5 h for prefreezing. The samples were subsequently transferred to a −20°C refrigerator for 20 min and sliced into 15-μm sections with a Leica CM1950 cryostat (Leica, Germany) at −20°C. The slices were subsequently mounted on the conductive side of an indium tin oxide (ITO)-coated glass slide (Bruker, USA). Thereafter, the slide was dried and fitted into the metal frame designed for the Shimadzu iMScope QT.

2.3.2 | MSI Measurement

CHCA powder was heated to sublimation and deposited on the surface of the slide at 0.7 μm using a Shimadzu iMLayer. The slide was then installed on an iMScope QT. The mass range was set at 50–500 *m/z*, allowing us to detect targeted lignans. The mass resolution was set at 30 000. The spatial resolution was controlled at 10 μm × 10 μm. The samples were scanned with a 10-μm laser diameter, the laser power was optimised at 60, and the repetition rate was 2000 Hz. The detector voltage was set at 2.2 kV. The Shimadzu IMAGEREVEAL MS software was used to manually select the region of interest, which represents the scanning area, according to the shapes of the tested samples under the optical microscope integrated with the iMScope

QT. All the acquired data were subsequently analysed via IMAGEREVEAL MS software.

2.4 | Py-GC/MS Analysis

One single seed was separated into two parts: the embryo part and the testa-endosperm part. A picture of the tested parts is provided in the Supporting Information (Figure S1). We then placed two samples into different stainless steel sample cups and loaded them on a Py-GC/MS instrument, a NexisGC2030 gas chromatograph linked with a Shimadzu QP2020 NX quadrupole mass spectrometer, with a Frontier Laboratories PY-3030D connected to the GC injection port. The column was a Frontier Laboratories Ultra ALLOY5 fused silica capillary column (30 m length, 0.25 mm inner diameter and coated with a 0.25 μm film thickness). The test protocol was described in our previous work with minor modifications [41]. In brief, the parameters of the GC were as follows: furnace, 350°C; Py-GC interface, 350°C; oven temperature, 40°C for 3 min, ramped to 325°C at 10 min^{-1}, 325°C for 10 min; carrier gas, nitrogen at 1 $mL \cdot min^{-1}$; injector temperature, 300°C; split mode ratio, 1:20. The parameters of the mass spectrometer were as follows: scan range, 40–550 u; electron ionisation voltage, 70 eV; interface temperature, 250°C; and MS source temperature, 200°C.

3 | Results and Discussion

3.1 | Microscopic Observation

A quick screen via microscopic observation confirmed that the analysed ancient samples were in good condition (Figures 1c–e and S2). The analysed samples were similar to pears in shape, with one end slightly pointed and an oval shape in cross section. Narrow ridges around the circumference are evident on the seeds, whose colour varies from beige to dark brown. Therefore, the seeds were morphologically identified as sesame seeds [41]. The anatomy of the seeds is shown in Figure 2. The three parts of sesame seeds are testa (seed coat, a single layer of cells), endosperm (two to five layers of cells) and embryo (with large cotyledons) [36].

The raw, roasted, homemade stir-fried modern sesame seeds as well as ancient samples from the same archaeological unit were subsequently observed via a Phenom ProX scanning electric microscope (SEM). Briefly, the granules on the surfaces were more pronounced on both ancient and modern roasted sesame seeds (Figure S2). Previously tested 10 ancient sesame seeds also presented similar granular surfaces [41]. Interestingly, the granules were invisible in the slightly stir-fried samples compared with those in the raw seeds (Figure S2). As the stir-frying time increased, the granules became more noticeable. Nevertheless, different kinds of sesame seeds may present different morphological traits, and the detailed surface changes resulting from roasting await further research.

Microcomputed tomography (μ-CT) is one of the most widely used nondestructive methods for obtaining the surface and inner structure of a wide range of samples [61]. The μ-CT analysis revealed that the inner structure of the sesame seeds was well preserved and was comparable to that of modern samples (Figure 3). The testa, endosperm and embryo can be clearly visualised in all ancient and modern samples. We also found that ancient samples exhibited nearly negligible cavities between embryos and endosperms (Figure 3a–c), in contrast to modern seeds where pronounced cavities were observed in these two parts (Figure 3d–f), which indicated that the ancient samples were crushed. In summary, screening via observations indicated that MSI could be well conducted.

3.2 | Test Condition Optimisation

Lignans are dimers that play important roles in plant physiology, and their basic structure is C_6-C_3 [40, 62, 63]. Sesamin and sesamolin are furofuran lignans containing two 1,3-benzodioxole groups and a tetrahydro-1H,3H-furo[3,4-c]furan skeleton [38, 39, 64]. Sesamol is a benzodioxole [37] and is considered to be related to the high oxidative rancidity of sesame oil [65]. The molecular weights (exact masses) of sesamin, sesamolin and sesamol are 354.11034, 370.10525 and 138.03169 g/mol, respectively.

According to previous studies, the same substrates could have different ionising capacities when different matrix compounds are used [24, 28]. To find the optimised matrix for our analytes, the MSI matrices of DHB, CHCA, 1,5-DAN, 9AA, NEDC, DHAP, DCTB and DI were tested. The sesamin, sesamol and sesamolin were dissolved in methanol to 1000 mg/L to prepare a standard solution with 10 mg/L of these three lignans. The matrices DHB, CHCA, 9AA, 1,5-DAN, NEDC, DHAP, DCTB and DI were dissolved in 70% methanol to 10 mg/L, while 1,5-DAN was dissolved in dichloromethane to 10 mg/L. A total of 0.5 μL of standard solution and 1 μL of matrix solution were mixed on a FlexiMass-SR48 steel target plate (P/N: TO-431R00, Shimadzu, Japan), and the plate was dried and loaded on a Shimadzu iM-Scope QT to search for the best testing conditions.

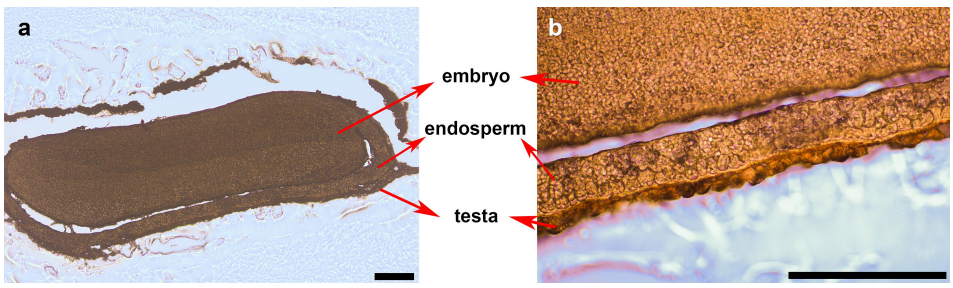

FIGURE 2 | Structure of a mature seed of *Sesamum indicum* L. Images were obtained with a Leica DM4 P. 1 bar = 250 μm.

The optimisation results revealed that the highest sensitivity of the signal was detected in positive mode for DHB and CHCA (Figures 4 and S3). However, 1,5-DAN and 9AA worked better in negative mode (Figures 4 and S4). Although 1,5-DAN was proven to be the most suitable matrix for visualising sesamin and sesamolin, it did not work well on sesamol. Moreover, the NEDC and DHAP were also not optimal choices for detecting sesamol (Figure S4). Comparatively, the CHCA matrix showed good ionising capacity for simultaneously detecting the three targeted lignans. Therefore, the CHCA matrix was chosen as the matrix, and sesamin, sesamolin and sesamol were detected as $[M\text{-}e]^+$ ions at m/z 354.110 ± 0.004, $[M\text{-}e]^+$ ions at m/z 370.105 ± 0.004 and $[M\text{-}e]^+$ ions at m/z 138.031 ± 0.001, respectively, for MSI analysis.

3.3 | Distribution of Lignans in Sesame Seeds

Sesame is a significant agricultural and economic plant. Our previous work pioneered the successful application of analytical pyrolysis and solvent extraction approaches to characterise sesame biomarkers in ancient sesame (sesamol, sesamin and sesamolin) [41]. In fact, sesame lignans have drawn increasing

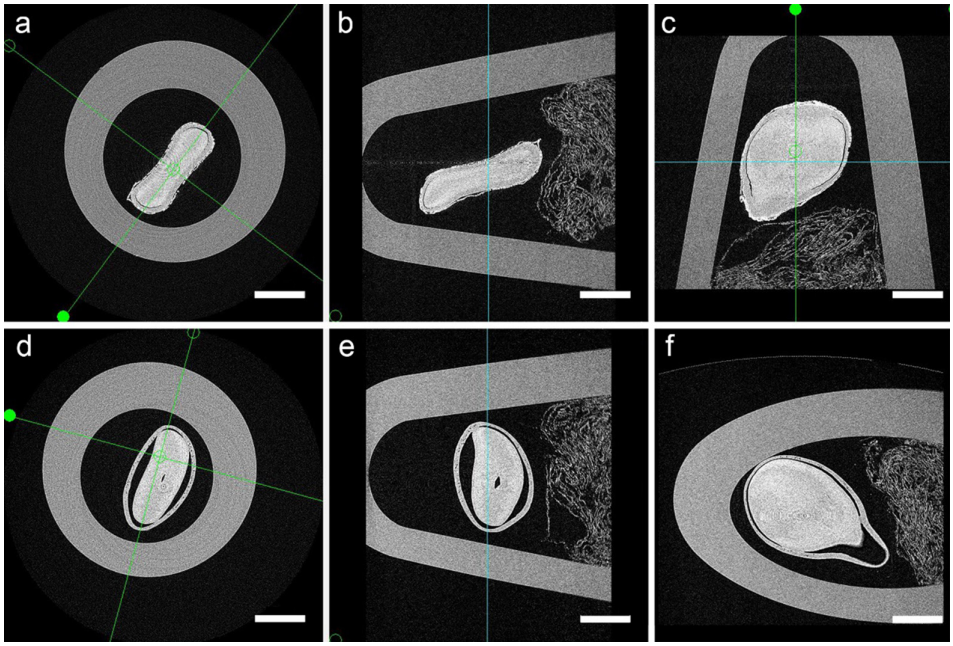

FIGURE 3 | μCT analysis of ancient and modern sesame seeds. (a–c) μCT image of an ancient sample; (d–f) μCT image of a modern sample. Images were obtained using a Shimadzu inspeXio SMX-225CT FPD HR Plus high-performance microfocus X-ray CT system. 1 bar = 1 mm.

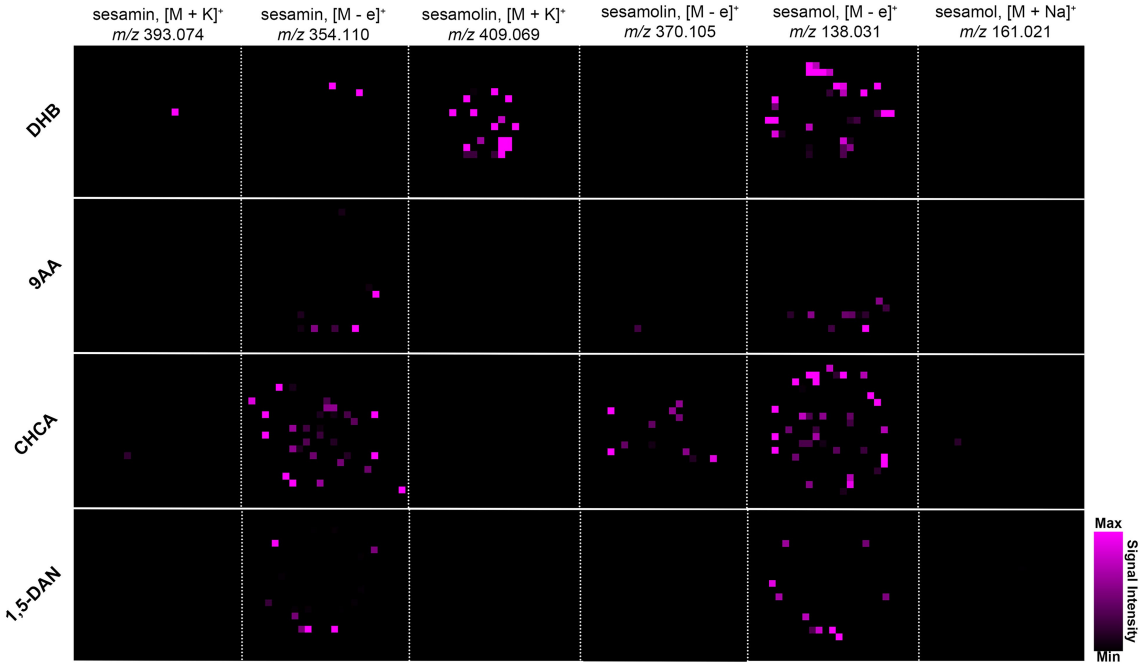

FIGURE 4 | Test results of positive modes using the DHB, 9AA, CHCA and 1,5-DAN matrices.

attention as a result of their potential medical and pharmacological benefits [66, 67]. Although several other species are listed on LOTUS (an online database for natural products), which are capable of synthesising sesamin or sesamolin [68], their concentrations are lower than those reported in sesame [67, 69]. Moreover, sesame oil is the only edible oil that contains sesamin or sesamolin [69]. Consequently, further detailed information about these lignans would contribute to a deeper understanding of their biosynthesis and ancient sesame use.

The distributions of targeted lignans in sesame seeds were studied. The signal intensity (SNI) scales for the MSI images of sesamin, sesamolin and sesamol were all set at 0–10. Generally, as illustrated in Figure 5, the signals of sesamin and sesamolin were present mainly in the cavities where the testa was well separated from the endosperm in both roasted and raw modern sesame seeds. In the embryo part, the SNIs of sesamin and sesamolin were sparsely distributed with lower intensities than those in the cavity parts. The SNIs of the analytes were highest in MU01, which also possessed the largest cavity among all the tested samples. In MU02, there was a clear line between the high sesamin SNI area and no signal area. It was also the boundary between the embryo and the cavity. In MU03, the signals of analytes also appeared at embryo fracture. The SNIs in MB01 were relatively low. There were no obvious signals of sesamin or sesamolin in the fractures of the embryos. The highest sesamin

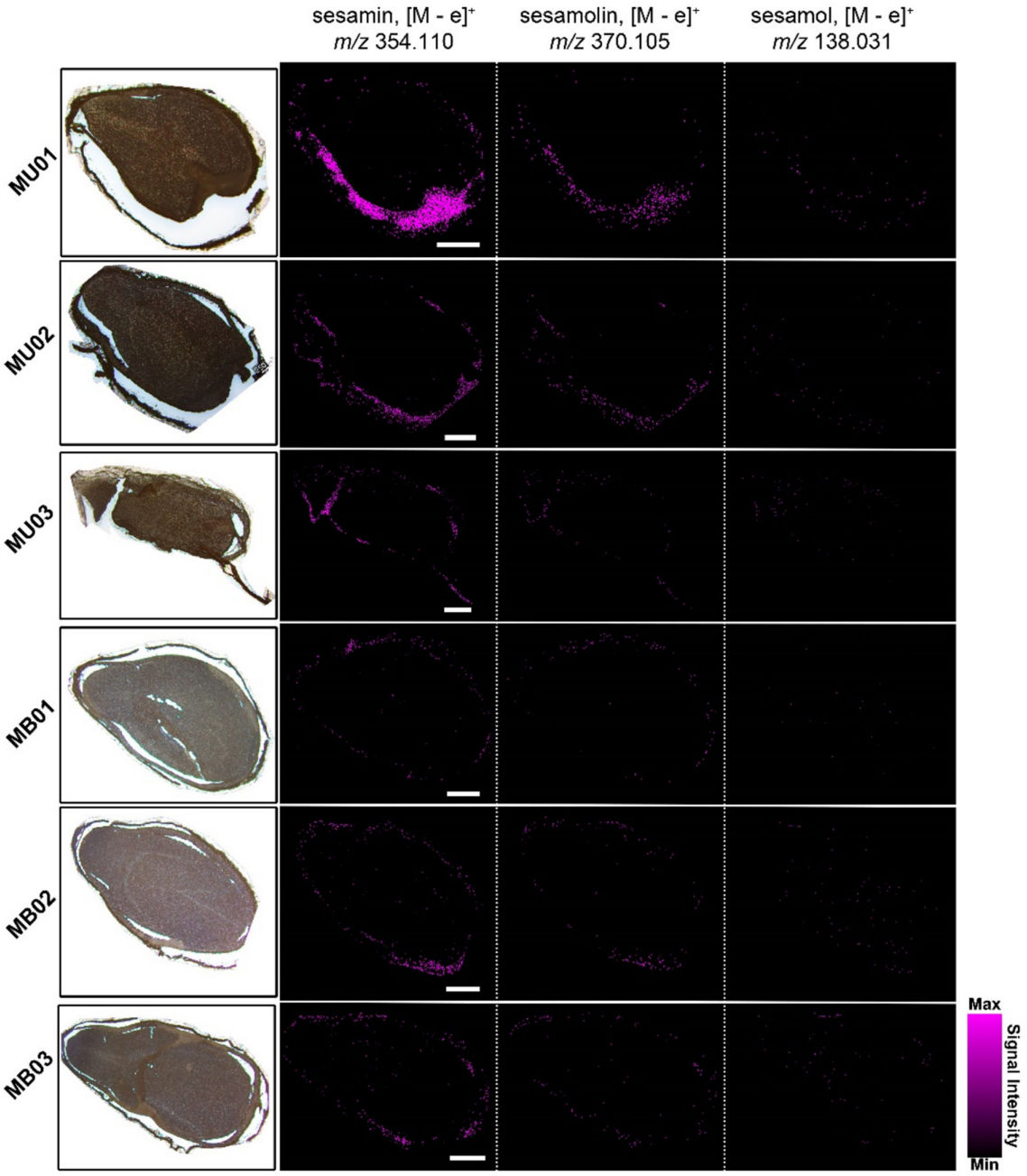

FIGURE 5 | Distribution of sesamin, sesamolin and sesamol in modern samples. 1 bar = 500 μm. MU refers to raw seeds, whereas MB refers to roasted seeds.

SNI areas in MB02 appeared at the largest cavities at the bottom-right of the image. In all the roasted samples, we detected sesamol signals in the embryo parts.

With respect to plant physiology, studies have investigated how fermentation and physical and/or chemical treatments affect the distribution of compounds, including some biomarkers [28, 29]. The characteristic distribution of certain compounds reflects changes in the outer and/or inner conditions of the plant. Similarly, MALDI-MSI has been applied to fresh and processed food to detect differences between the same samples subjected to different treatments [70]. The localisation of low molecular weight (LMW) biomarkers is one of the most important criteria. Nevertheless, using MALDI-MSI to visualise the distribution of LMW biomarkers is challenging. According to previous studies, the localisation of LMW compounds can be affected by matrices, salts, lipids and other compounds [71–74]. Various strategies have been developed to improve the performance of LMW compounds, such as the use of different mass spectrometers, different ionisation strategies, the introduction of new matrices, the application of cleanup protocols and the chemical derivatisation of samples [74].

In this study, one single sesame seed was separated, and Py-GC/MS was carried out to further investigate the possible influences of other substitutes in the MSI analysis of lignans, as rarely tested lignans were observed in the embryo. As shown in Figure 6, sesamin, sesamolin and sesamol were identified in both embryo and testa-endosperm parts. Sesamin, sesamolin and sesamol were detected with main peaks at *m/z* 149, 135 and 138, respectively (Figures S5–S7), indicating that these analytes were localised in both the embryo and testa-endosperm parts of sesame seeds. The pyrolysis of sesame seed parts confirmed that sesame lignans exist in the embryo, testa-endosperm parts (the endosperm is thin and difficult to separate from the testa). Notably, pyrolysis results in a high oil content (especially $C_{18:2}$ in Figure 6a), which is in accordance with previous studies [36, 43, 75, 76]. Lipids are among the most common factors affecting the results of MALDI-MSI [77].

In addition, the TIC images of the MSI tests also showed that the signal in the embryo parts was not good (Figure S8). Thus, the detectable lignan signals were confined to the cavities between the embryo and testa, where these lignans peeled off into these cavities during the sectioning process with little lipid interference during the MALDI desorption process.

3.4 | MSI in Visualising Characteristic Biomarkers That Aids Archaeological Interpretations

The MSI results of ancient sesame seeds revealed that the distributions of sesamin and sesamolin were similar to those of modern samples. In brief, they also appeared mainly at the cavities between the testa and the endosperm (Figure 7). There were no obvious signals of our analytes in the embryo parts of the samples. In all three ancient seeds, the SNIs of sesamin and sesamolin mainly accumulated at one side of the samples where the cavities were relatively large, which proved that the lignans were still detectable after thousand years of burial. Lipid inhibition also occurred in ancient seeds. For AN02, the signals of sesamin and sesamolin were relatively strong at the testa of the pointed edge of the seed. In terms of sesamol, only a few dots indicated its presence, which meant that sesamol might have degraded during the long period of preservation.

Notably, non-targeted MSI analysis also provided more information in addition to the above targeted lignan analysis. For example, different patterns of an unattributed compound (CP1) with *m/z* 393.074 ± 0.004 were observed between the roasted and raw samples. As shown in Figure 8, there were more 'signal dots' in the embryos of the raw seeds than in those of the roasted seeds, which implied that the signals of CP1 in the embryo were more densely distributed in the raw sesame seeds than in the roasted seeds. Then, we further checked the original MS data and found that the average CP1 intensities were more than 4 times higher in raw than in roasted seeds (Table S1). CP1 in the ancient sesame seeds exhibited a

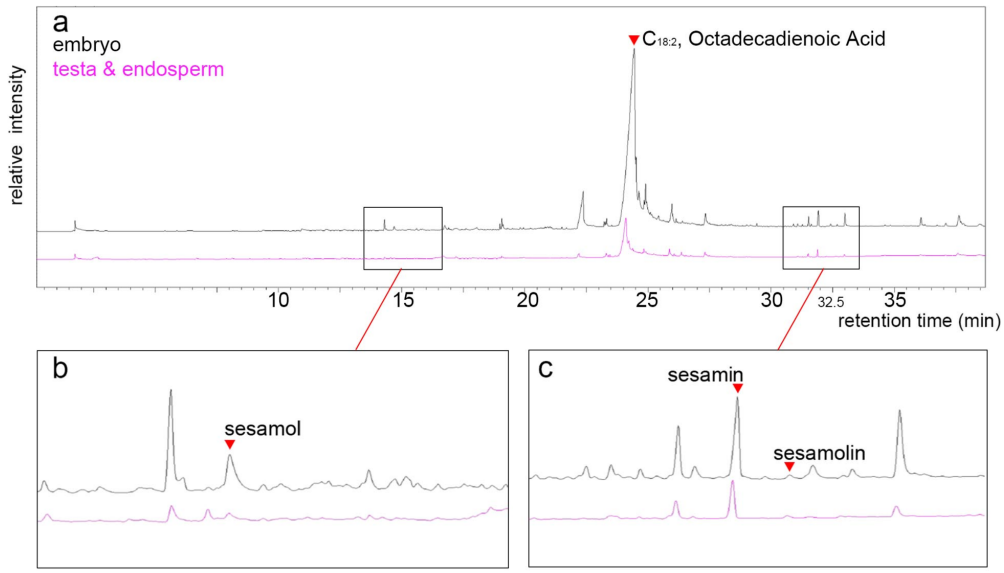

FIGURE 6 | Pyrolysis results of different parts of modern sesame seed; pink curves referred to embryo part of modern sesame seed, and black curves referred to testa-endosperm parts of modern sesame seed. (a) Total ion current (TIC) chromatograms of different parts of sesame seed. (b) Magnified TIC chromatogram indicating the peak of sesamol. (c) Magnified TIC chromatogram indicating the peaks of sesamin and sesamolin.

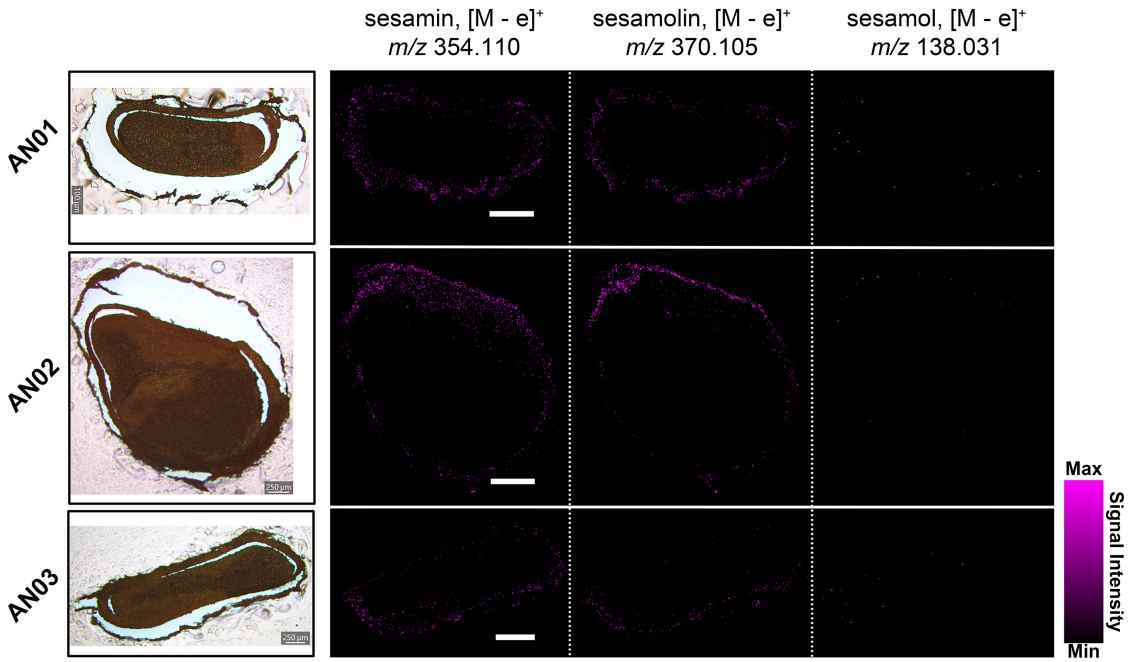

FIGURE 7 | Distributions of sesamin, sesamolin and sesamol in different ancient samples. 1 bar = 500 μm.

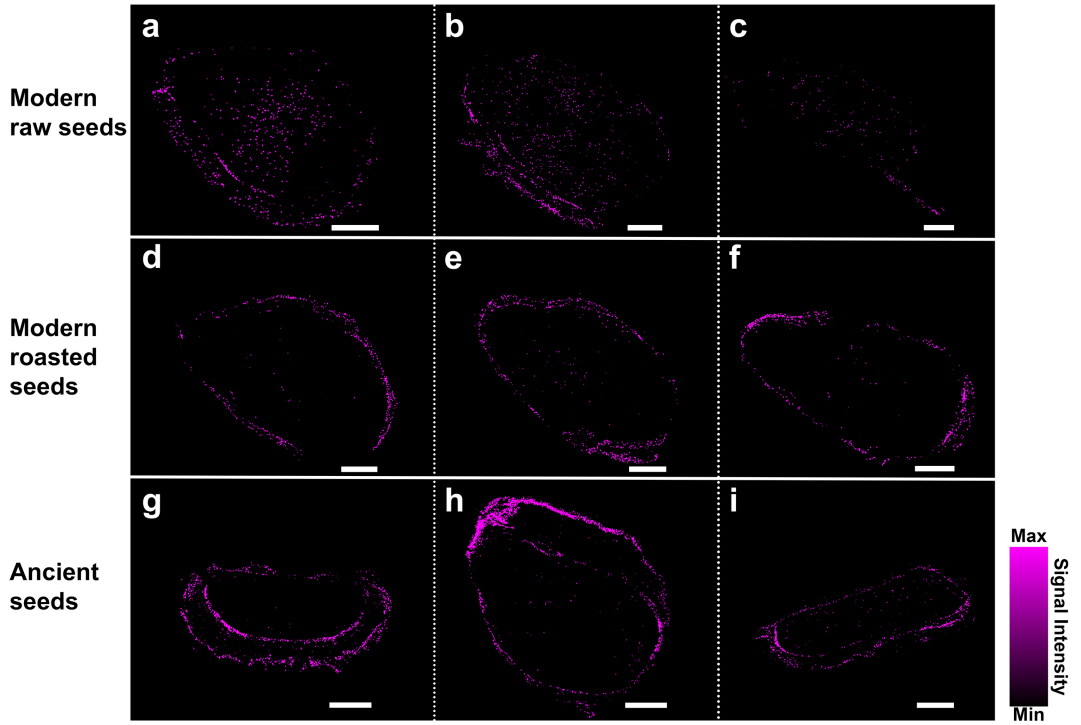

FIGURE 8 | Visualisation of the compound at *m/z* 393.074 ± 0.004. (a–c) Referred to MU01, MU02 and MU03, respectively. (d–f) Referred to MB01, MB02 and MB03, respectively. (g–i) Referred to AN01, AN02 and AN03, respectively. 1 bar = 500 μm.

similar distribution pattern to that of the roasted modern samples, showing that this difference can preliminarily be used to distinguish raw sesame seeds from roasted modern sesame seeds. This identification criterion was supplemented by SEM morphological changes introduced by roasting.

Moreover, historical and previous archaeological materials also shed some light on interpretations of the use of these sesame seeds. In both historical and modern time, sesame seeds have usually been roasted to increase oil recovery [41, 78]. The sesame oil used for religious lamps was previously discovered in the Astana Cemetery [79]. It was dated back to the 6th to 8th centuries AD, which was contemporary archaeological samples compared with the ancient sesame seeds used in this study. In a previous study, some tested sesame seeds from the same archaeological unit were found to be broken [41]. This was in accordance with the μ-CT results, which implied that these ancient seeds could have been crushed. Furthermore, based

on textual materials from the Tang and Five Dynasties Period (618–960 AD) unearthed from Dunhuang (540 km southeast of Gaochang), northwest China, oil press devices were used during this period (Figure S9). The oil extraction efficiency of this device was rather low, which meant that the oil seeds would not be destroyed. Given that both Gaochang and Dunhuang belong to Hexi Dao (河西道, Dao was the first-level administrative division in the Tang Dynasty) or Longyou Dao (陇右道) in the Tang Dynasty [80]. They were connected by the Silk Road; the culture and technology exchanges between those two places were close at that time. Most important, textual record (Tang Dynasty) of oil press component was found in the Astana Cemetery. The same component also appeared in aforementioned textual materials from Dunhuang.

The research case demonstrated in this study illustrated the potential of MSI in visualising characteristic biomarkers and provides more insights into our archaeological interpretations. As noted, different plant species may present similar morphological traits that greatly hinder their identification in archaeobotanical practice. MSI is a powerful spectral fingerprint tool that enables rapid screening of multiple compounds in one single test. The MS data in whole and specific parts of the samples can all be accessed in MSI tests during postprocessing, while MS analysis usually obtains only the former [81]. Conversely, it is noteworthy to observe morphologically dissimilar species that produced similar mass spectra [81, 82]. In this case, the combination of MSI with different analytical techniques and the exploration of different analytical strategies have the potential to demonstrate the advantages of in visualising different compound distributions with similar mass spectra produced by different mechanisms [22, 31, 83].

4 | Conclusions

Archaeobotanical material studies constitute an important part of archaeological research, and the characterisation of characteristic biomarkers helps in understanding ancient plant use and human adaptation to environmental change. In this study, the MSI traits of modern and ancient sesame seeds were studied to explore archaeobotanical findings through the characterisation of sesame lignans. The MSI distributions of sesamin and sesamolin were similar in modern and ancient sesame seeds, whereas their MSI signals were inhibited by lipidic substances in the in situ MSI tests. Furthermore, non-targeted MSI analysis has the potential to reveal plant material treatment processes, in addition to targeted biomarker characterisation. MSI technology has, for the first time, been applied in archaeological/archaeobotanical studies, demonstrating its potential in detecting and localising characteristic biomarkers in archaeobotanical materials and paves the way for other cereal/economical plant remains study in archaeological finds.

Author Contributions

Huanxi Li: writing – original draft, writing – review and editing, validation, methodology, investigation, visualization, formal analysis. **Bin Han:** funding acquisition, writing – original draft, writing – review and editing, project administration, methodology, conceptualization, supervision, resources, validation, data curation, investigation, visualization. **Hongen Jiang:** writing – review and editing, validation, resources, investigation. **Bo Wang:** resources, writing – review and editing, investigation. **Mengxuan Chen:** methodology, software, writing – review and editing, data curation, visualization. **Mianbo Ning:** software, data curation, writing – review and editing. **Yimin Yang:** writing – review and editing, validation, conceptualization, project administration, investigation.

Acknowledgements

This study was supported by the Beijing Social Science Foundation Young Academic Leader Project (24DTR077), the National Natural Science Foundation of China (42202211) and the Scientific and Technological Research Projects on Cultural Heritage (2023ZCK008).

Conflicts of Interest

The authors declare no conflicts of interest.

Data Availability Statement

The data that support the findings of this study are available from the corresponding author upon reasonable request.

References

1. A. C. D'Andrea, *Palaeoethnobotany* (Cambridge University Press, 2019), 276–313, https://doi.org/10.1017/9781139013826.012.

2. A. De Vareilles, R. Pelling, J. Woodbridge, and R. Fyfe, "Archaeology and Agriculture: Plants, People, and Past Land-Use," *Trends in Ecology & Evolution* 36, no. 10 (2021): 943–954, https://doi.org/10.1016/j.tree.2021.06.003.

3. G. S. L. Stuart, *Paleoethnobotany* (Springer International Publishing, 2018), 1–16, https://doi.org/10.1007/978-3-319-51726-1_2412-2.

4. U. Herzschuh, X. Cao, T. Laepple, et al., "Position and Orientation of the Westerly Jet Determined Holocene Rainfall Patterns in China," *Nature Communications* 10, no. 1 (2019): 2376, https://doi.org/10.1038/s41467-019-09866-8.

5. K. Mausolf, W. Härdtle, K. Jansen, et al., "Legacy Effects of Land-Use Modulate Tree Growth Responses to Climate Extremes," *Oecologia* 187, no. 3 (2018): 825–837, https://doi.org/10.1007/s00442-018-4156-9.

6. S. Sugita, "Pollen Representation of Vegetation in Quaternary Sediments: Theory and Method in Patchy Vegetation," *Journal of Ecology* 82, no. 4 (1994): 881, https://doi.org/10.2307/2261452.

7. A. Bogaard, R. Krause, and H.-C. Strien, "Towards a Social Geography of Cultivation and Plant Use in an Early Farming Community: Vaihingen an der Enz, South-West Germany," *Antiquity* 85, no. 328 (2011): 395–416, https://doi.org/10.1017/s0003598x00067831.

8. T. Chen, X. Wang, J. Dai, W. Li, and H. Jiang, "Plant Use in the lop nor Region of Southern Xinjiang, China: Archaeobotanical Studies of the Yingpan Cemetery (~25–420 AD)," *Quaternary International* 426 (2016): 166–174, https://doi.org/10.1016/j.quaint.2016.03.015.

9. N. Lyu, Y. Li, S. Yang, et al., "Microdestructive Analysis With Py-GC/MS for the Identification of Birch Tar: A Case Study From the Huayang Site in Late Neolithic China," *European Physical Journal Plus* 138, no. 7 (2023): 580.

10. X. Li, X. Shang, J. Dodson, and X. Zhou, "Holocene Agriculture in the Guanzhong Basin in NW China Indicated by Pollen and Charcoal Evidence," *Holocene* 19, no. 8 (2009): 1213–1220, https://doi.org/10.1177/0959683609345083.

11. G. Zhang, X. Zhou, X. Li, et al., "New Empirical Evidence From Ancient Foxtail Millet Seeds and Panicles Reveals Phenotype Divergence

During Its Dispersal," *Science Bulletin* 67, no. 18 (2022): 1860–1864, https://doi.org/10.1016/j.scib.2022.08.015.

12. C. E. Peterson and G. Shelach, "Jiangzhai: Social and Economic Organization of a Middle Neolithic Chinese Village," *Journal of Anthropological Archaeology* 31, no. 3 (2012): 265–301, https://doi.org/10.1016/j.jaa.2012.01.007.

13. P. Sheng, X. Shang, X. Zhou, et al., "Feeding Shimao: Archaeobotanical and Isotopic Investigation Into Early Urbanism (4200-3000 BP) on the Northern Loess Plateau, China," *Environmental Archaeology* 29, no. 5 (2021): 425–439, https://doi.org/10.1080/14614103.2021.2009995.

14. M. Ge, Z. Gu, F. Tian, et al., "Scientific Analysis of Folk Contract Documents From Tianshui Region: Insights of Fiber Use and Preservation State," *Heritage Science* 12, no. 1 (2024): 289.

15. B. Han, J. Vial, S. Sakamoto, and M. Sablier, "Identification of Traditional East Asian Handmade Papers Through the Multivariate Data Analysis of Pyrolysis-GC/MS Data," *Analyst* 144, no. 4 (2019): 1230–1244, https://doi.org/10.1039/C8AN01898G.

16. J. Dunne, A. M. Mercuri, R. P. Evershed, S. Bruni, and S. di Lernia, "Earliest Direct Evidence of Plant Processing in Prehistoric Saharan Pottery," *Nature Plants* 3, no. 1 (2016): 16194, https://doi.org/10.1038/nplants.2016.194.

17. B. Han, J. Niang, H. Rao, et al., "Paper Fragments From the Tibetan Samye Monastery: Clues for an Unusual Sizing Recipe Implying Wheat Starch and Milk in Early Tibetan Papermaking," *Journal of Archaeological Science: Reports* 36 (2021): 102793, https://doi.org/10.1016/j.jasrep.2021.102793.

18. R. P. Evershed, "Organic Residue Analysis in Archaeology: The Archaeological Biomarker Revolution*," *Archaeometry* 50, no. 6 (2008): 895–924, https://doi.org/10.1111/j.1475-4754.2008.00446.x.

19. B. Han, Z. Sun, J. Chong, N. Lyu, H. Rao, and Y. Yang, "Lipid Residue Analysis of Ceramic Vessels From the Liujiawa Site of the Rui State (Early Iron Age, North China)," *Journal of Quaternary Science* 37, no. 1 (2022): 114–122, https://doi.org/10.1002/jqs.3377.

20. M. Ren, Z. Tang, X. Wu, et al., "The Origins of Cannabis Smoking: Chemical Residue Evidence From the First Millennium BCE in the Pamirs," *Science Advances* 5, no. 6 (2019): eaaw1391, https://doi.org/10.1126/sciadv.aaw1391.

21. S. Wei, X. Fang, X. Cao, and M. Schreiner, "Characterization of the Materials Used in Chinese Ink Sticks by Pyrolysis-Gas Chromatography–Mass Spectrometry," *Journal of Analytical and Applied Pyrolysis* 91, no. 1 (2011): 147–153, https://doi.org/10.1016/j.jaap.2011.02.001.

22. W. Lu, J. Wang, Y. Xie, S. Wu, L. Li, and H. Xu, "Mass Spectrometry Imaging: An Emerging Technology in Plant Molecular Physiology," *Phytochemistry Reviews* 23 (2023): 551–577, https://doi.org/10.1007/s11101-023-09898-5.

23. B. Spengler, "Mass Spectrometry Imaging of Biomolecular Information," *Analytical Chemistry* 87, no. 1 (2015): 64–82, https://doi.org/10.1021/ac504543v.

24. A. Svatoš, "Mass Spectrometric Imaging of Small Molecules," *Trends in Biotechnology* 28, no. 8 (2010): 425–434, https://doi.org/10.1016/j.tibtech.2010.05.005.

25. A. R. Buchberger, K. Delaney, J. Johnson, and L. Li, "Mass Spectrometry Imaging: A Review of Emerging Advancements and Future Insights," *Analytical Chemistry* 90, no. 1 (2018): 240–265, https://doi.org/10.1021/acs.analchem.7b04733.

26. L. A. McDonnell and R. M. A. Heeren, "Imaging Mass Spectrometry," *Mass Spectrometry Reviews* 26, no. 4 (2007): 606–643, https://doi.org/10.1002/mas.20124.

27. K. Chughtai and R. M. A. Heeren, "Mass Spectrometric Imaging for Biomedical Tissue Analysis," *Chemical Reviews* 110, no. 5 (2010): 3237–3277, https://doi.org/10.1021/cr100012c.

28. S. Kaspar, M. Peukert, A. Svatos, A. Matros, and H. P. Mock, "MALDI-Imaging Mass Spectrometry—An Emerging Technique in Plant Biology," *Proteomics* 11, no. 9 (2011): 1840–1850, https://doi.org/10.1002/pmic.201000756.

29. D. R. Bhandari, Q. Wang, W. Friedt, B. Spengler, S. Gottwald, and A. Römpp, "High Resolution Mass Spectrometry Imaging of Plant Tissues: Towards a Plant Metabolite Atlas," *Analyst* 140, no. 22 (2015): 7696–7709, https://doi.org/10.1039/c5an01065a.

30. A. E. Kramell, M. García-Altares, M. Pötsch, et al., "Mapping Natural Dyes in Archeological Textiles by Imaging Mass Spectrometry," *Scientific Reports* 9, no. 1 (2019): 2331, https://doi.org/10.1038/s41598-019-38706-4.

31. S. Hammann, D. J. Scurr, M. R. Alexander, and L. J. E. Cramp, "Mechanisms of Lipid Preservation in Archaeological Clay Ceramics Revealed by Mass Spectrometry Imaging," *Proceedings of the National Academy of Sciences* 117, no. 26 (2020): 14688–14693, https://doi.org/10.1073/pnas.1922445117.

32. J. Dekker, T. Larson, J. Tzvetkov, et al., "Spatial Analysis of the Ancient Proteome of Archeological Teeth Using Mass Spectrometry Imaging," *Rapid Communications in Mass Spectrometry* 37, no. 8 (2023): e9486, https://doi.org/10.1002/rcm.9486.

33. A. Adriaens and M. G. Dowsett, "Applications of SIMS to Cultural Heritage Studies," *Applied Surface Science* 252, no. 19 (2006): 7096–7101, https://doi.org/10.1016/j.apsusc.2006.02.127.

34. C. Bouvier, S. Van Nuffel, P. Walter, and A. Brunelle, "Time-of-Flight Secondary Ion Mass Spectrometry Imaging in Cultural Heritage: A Focus on old Paintings," *Journal of Mass Spectrometry* 57, no. 1 (2022): e4803, https://doi.org/10.1002/jms.4803.

35. K. Keune and J. J. Boon, "Imaging Secondary Ion Mass Spectrometry of a Paint Cross Section Taken From an Early Netherlandish Painting by Rogier van der Weyden," *Analytical Chemistry* 76, no. 5 (2004): 1374–1385, https://doi.org/10.1021/ac035201a.

36. J. G. Vaughan, *The Structure and Utilization of Oil Seeds* (Richard Clay (The Chancer Press Ltd, 1970).

37. NCBI (National Center for Biotechnology Information), *PubChem Compound Summary for CID 68289, 3,4-Methylenedioxyphenol* (PubChem, 2024), Retrieved July 31 from, https://pubchem.ncbi.nlm.nih.gov/compound/3_4-Methylenedioxyphenol.

38. NCBI (National Center for Biotechnology Information), *PubChem Compound Summary for CID 72307 Sesamin* (PubChem, 2024), Retrieved July 31 from, https://pubchem.ncbi.nlm.nih.gov/compound/Sesamin.

39. NCBI (National Center for Biotechnology Information)), *PubChem Compound Summary for CID 585998, (+)-Sesamolin* (Pub-Chem, 2024). Retrieved July 31 from, https://pubchem.ncbi.nlm.nih.gov/compound/585998.

40. M. M. Vuolo, V. S. Lima, and M. R. Maróstica Junior, *Phenolic Compounds: Structure, Classification, and Antioxidant Power* (Elsevier, 2019), 33–50, https://doi.org/10.1016/b978-0-12-814774-0.00002-5.

41. T. Chen, B. Wang, Y. Yang, B. Han, and H. Jiang, "Sesame Use in Turpan During the Tang Dynasty: Evidence From the Astana Cemetery," *Journal of Archaeological Science: Reports* 53 (2024): 104298, https://doi.org/10.1016/j.jasrep.2023.104298.

42. N. M. Nayar, K. L. Mehra, N. M. Nayar, and K. L. Mehra, "Sesame: Its Uses, Botany, Cytogenetics, and Origin," *Economic Botany* 24, no. 1 (1970): 20–31, https://doi.org/10.1007/BF02860629.

43. Z. Qiu, Y. Zhang, D. Bedigian, X. Li, C. Wang, and H. Jiang, "Sesame Utilization in China: New Archaeobotanical Evidence From Xinjiang," *Economic Botany* 66, no. 3 (2012): 255–263, https://doi.org/10.1007/s12231-012-9204-5.

44. D. Bedigian and J. R. Harlan, "Evidence for Cultivation of Sesame in the Ancient World," *Economic Botany* 40, no. 2 (1986): 137–154, https://doi.org/10.1007/bf02859136.

45. Z.-Y. Wu, "Huma Should Be *Linum usitatissimum*, Not *Sesamum indicum*—With Special Reference to the Source of Confusion of Names for Traditional Chinese Medicine and the Written Time and Author of Shên Nung Pên Ts'ao Ching," *Acta Phytotaxonomica Sinica* 45, no. 4 (2007): 458, https://doi.org/10.1360/aps06196.

46. S. Gao, M. Yao, D. Guo, et al., "Identification of Fibers and Dyes in Archaeological Textiles From Bazhou, Xinjiang (220-420 CE), and Their Silk Road Origins," *Journal of Archaeological Science* 164 (2024): 105941, https://doi.org/10.1016/j.jas.2024.105941.

47. H.-E. Jiang, X. Li, Y.-X. Zhao, et al., "A New Insight Into *Cannabis sativa* (Cannabaceae) Utilization From 2500-Year-Old Yanghai Tombs, Xinjiang, China," *Journal of Ethnopharmacology* 108, no. 3 (2006): 414–422, https://doi.org/10.1016/j.jep.2006.05.034.

48. H. Wang, J. Chen, M. Qiu, et al., "Climate Change Drove the Route Shift of the Ancient Silk Road in Two Distinct Ways," *Science Bulletin* 69, no. 8 (2024): 1153–1160, https://doi.org/10.1016/j.scib.2024.02.025.

49. L. Wang, G. Ren, B. Han, and Y. Yang, "Characterization of Lamp Oil Residues From Tangchaodun Site, Xinjiang, Northwest China During the 8th–13th Centuries CE," *Journal of Archaeological Science: Reports* 56 (2024): 104574, https://doi.org/10.1016/j.jasrep.2024.104574.

50. W. Wang, M. Ding, J. D. Gardner, et al., "Ancient Xinjiang Mitogenomes Reveal Intense Admixture With High Genetic Diversity," *Science Advances* 7, no. 14 (2021): eabd6690, https://doi.org/10.1126/sciadv.abd6690.

51. S. Xu, B. Wang, B. Han, and Y. Yang, "The Production of Indo-Pacific Monochrome Drawn Glass Beads in the Sasanian Empire: Insights From Xinjiang, Northwest China," *Ceramics International* 48, no. 18 (2022): 26055–26062, https://doi.org/10.1016/j.ceramint.2022.05.287.

52. S. Zhang, H. Liu, G. Li, et al., "Warfare Impact Overtakes Climate-Controlled Fires in the Eastern Silk Roads Since 2000 B.P," *PNAS Nexus* 2, no. 12 (2023): pgad408, https://doi.org/10.1093/pnasnexus/pgad408.

53. X. Zhou, J. Yu, R. N. Spengler, et al., "5,200-Year-Old Cereal Grains From the Eastern Altai Mountains Redate the Trans-Eurasian Crop Exchange," *Nature Plants* 6, no. 2 (2020): 78–87, https://doi.org/10.1038/s41477-019-0581-y.

54. M. Qiu, R. Liu, X. Li, et al., "Earliest Systematic Coal Exploitation for Fuel Extended to ~3600 B.P," *Science Advances* 9, no. 30 (2023): eadh0549, https://doi.org/10.1126/sciadv.adh0549.

55. S. Xu, Y. Luo, Z. Li, Y. Hou, N. Liu, and Y. Yang, "Adoption and Adaption: The Rise of Pb-Ba Glass Underlines the Impact of Soda Glass Along the Pre-Silk Road," *Science Bulletin* 70, no. 2 (2024): 172–175.

56. B. Han, N. Lyu, X. Chen, et al., "Hearth Residue Analysis Reveals Human Adaptation to the Younger Dryas on the Northeastern Qinghai-Tibetan Plateau," *Environmental Archaeology* (2023): 1–14, https://doi.org/10.1080/14614103.2023.2286119.

57. N. Lyu, T. Wang, J. Yu, H. Rao, B. Han, and Y. Yang, "Pottery Lipid Analysis at the Shangzhai Site, Beijing, and Its Implication for Subsistence Strategy," *Science China Earth Sciences* 66, no. 8 (2023): 1789–1797, https://doi.org/10.1007/s11430-022-1121-4.

58. N. Sun, Q. Ma, B. Han, and Y. Yang, "New Insights Into the Subsistence Strategies of the Northwest Frontier of the Western Zhou Dynasty (1046–771 BCE) Through Pottery Lipid Analysis," *Archaeological and Anthropological Sciences* 15, no. 6 (2023): 80.

59. B. Han, N. Lyu, L. Yan, et al., "Rapid Screening of Pottery Lipid Residue Profile via Comprehensive Two-Dimensional Gas Chromatography," *Analytica Chimica Acta* 1338 (2024): 343598, https://doi.org/10.1016/j.aca.2024.343598.

60. XIA (Xinjiang Institute of Archaeology), *Thirty Years of Archaeology in Xinjiang (In Chinese)* (Xinjiang People's Publishing House, 1983), http://refhub.elsevier.com/S2352-409X(23)00473-X/h0480.

61. Q. Wan, X. Li, W. Liu, Y. Li, B. Han, and T. Li, "Understanding the Manufacture of Hetian Administration Banknotes From Xinjiang Using Low- and High-Resolution Analytical Methods," *Studies in Conservation* 69, no. 7 (2024): 537–556, https://doi.org/10.1080/00393630.2024.2309423.

62. N. G. Lewis and L. B. Davin, *Lignans: Biosynthesis and Function* (Elsevier, 1999), 639–712, https://doi.org/10.1016/b978-0-08-091283-7.00027-8.

63. A. Zitterman, *Dietary Fiber|Bran* (Elsevier, 2003), 1844–1850, https://doi.org/10.1016/b0-12-227055-x/00346-1.

64. W. Worawalai, P. Khongchai, N. Surachaitanawat, and P. Phuwapraisirisan, "Synthesis of Furofuran Lignans as Antidiabetic Agents Simultaneously Achieved by Inhibiting α-Glucosidase and Free Radical," *Archives of Pharmacal Research* 39, no. 10 (2016): 1370–1381, https://doi.org/10.1007/s12272-016-0778-9.

65. M. A. Mujtaba, H. H. Masjuki, M. A. Kalam, et al., "Ultrasound-Assisted Process Optimization and Tribological Characteristics of Biodiesel From Palm-Sesame Oil via Response Surface Methodology and Extreme Learning Machine - Cuckoo Search," *Renewable Energy* 158 (2020): 202–214, https://doi.org/10.1016/j.renene.2020.05.158.

66. M. Andargie, M. Vinas, A. Rathgeb, E. Möller, and P. Karlovsky, "Lignans of Sesame (*Sesamum indicum* L.): A Comprehensive Review," *Molecules* 26, no. 4 (2021): 883, https://doi.org/10.3390/molecules26040883.

67. S. S. K. Dossou, F.-T. Xu, K. Dossa, R. Zhou, Y.-Z. Zhao, and L.-H. Wang, "Antioxidant Lignans Sesamin and Sesamolin in Sesame (*Sesamum indicum* L.): A Comprehensive Review and Future Prospects," *Journal of Integrative Agriculture* 22, no. 1 (2023): 14–30, https://doi.org/10.1016/j.jia.2022.08.097.

68. A. Rutz, M. Sorokina, J. Galgonek, et al., "The LOTUS Initiative for Open Knowledge Management in Natural Products Research," *eLife* 11 (2022): e70780, https://doi.org/10.7554/elife.70780.

69. D. Bedigian, D. S. Seigler, and J. R. Harlan, "Sesamin, Sesamolin and the Origin of Sesame," *Biochemical Systematics and Ecology* 13, no. 2 (1985): 133–139, https://doi.org/10.1016/0305-1978(85)90071-7.

70. J. Kokesch-Himmelreich, O. Wittek, A. M. Race, et al., "MALDI Mass Spectrometry Imaging: From Constituents in Fresh Food to Ingredients, Contaminants and Additives in Processed Food," *Food Chemistry* 385 (2022): 132529, https://doi.org/10.1016/j.foodchem.2022.132529.

71. M. Nishidate, M. Hayashi, H. Aikawa, et al., "Applications of MALDI Mass Spectrometry Imaging for Pharmacokinetic Studies During Drug Development," *Drug Metabolism and Pharmacokinetics* 34, no. 4 (2019): 209–216, https://doi.org/10.1016/j.dmpk.2019.04.006.

72. I. Rzagalinski and D. A. Volmer, "Quantification of Low Molecular Weight Compounds by MALDI Imaging Mass Spectrometry—A Tutorial Review," *Biochimica et Biophysica Acta (BBA) - Proteins and Proteomics* 1865, no. 7 (2017): 726–739, https://doi.org/10.1016/j.bbapap.2016.12.011.

73. J. Stauber, "Quantitation by Ms Imaging: Needs and Challenges in Pharmaceuticals," *Bioanalysis* 4, no. 17 (2012): 2095–2098, https://doi.org/10.4155/bio.12.187.

74. Z. Sun, F. Wang, Y. Liu, et al., "Recent Strategies for Improving MALDI Mass Spectrometry Imaging Performance Towards Low Molecular Weight Compounds," *TrAC Trends in Analytical Chemistry* 175 (2024): 117727, https://doi.org/10.1016/j.trac.2024.117727.

75. D. Bedigian, "Evolution of Sesame Revisited: Domestication, Diversity and Prospects," *Genetic Resources and Crop Evolution* 50, no. 7 (2003): 779–787, https://doi.org/10.1023/A:1025029903549.

76. D. M. Yermanos, W. Saleeb, S. Hemstreet, and C. K. Huszar, "Oil Content and Composition of the Seed in the World Collection of Sesame Introductions," *Journal of the American Oil Chemists' Society* 49, no. 1 (1972): 20–23, https://doi.org/10.1007/bf02545131.

77. E. Gemperline, B. Chen, and L. Li, "Challenges and Recent Advances in Mass Spectrometric Imaging of Neurotransmitters," *Bioanalysis* 6, no. 4 (2014): 525–540, https://doi.org/10.4155/bio.13.341.

78. M. L. Martínez, M. G. Bordón, R. L. Lallana, P. D. Ribotta, and D. M. Maestri, "Optimization of Sesame Oil Extraction by Screw-Pressing at Low Temperature," *Food and Bioprocess Technology* 10, no. 6 (2017): 1113–1121, https://doi.org/10.1007/s11947-017-1885-4.

79. A. Shevchenko, Y. Yang, A. Knaust, et al., "Open Sesame: Identification of Sesame Oil and Oil Soot Ink in Organic Deposits of Tang Dynasty Lamps From Astana Necropolis in China," *PLoS ONE* 12, no. 2 (2017): e0158636, https://doi.org/10.1371/journal.pone.0158636.

80. S. Guo, *A Comprehensive History of Chinese Administrative Divisions, the Tang Dynasty Volume [*中国行政区划通史·唐代卷*]* (Fudan University Press, 2012).

81. E. O. Espinoza, C. A. Lancaster, N. M. Kreitals, M. Hata, R. B. Cody, and R. A. Blanchette, "Distinguishing Wild From Cultivated Agarwood (*Aquilaria* spp.) Using Direct Analysis in Real Time and Time of-Flight Mass Spectrometry," *Rapid Communications in Mass Spectrometry* 28, no. 3 (2014): 281–289, https://doi.org/10.1002/rcm.6779.

82. E. R. Price, P. J. McClure, A. N. Huffman, D. Voin, and E. O. Espinoza, "Reliability of Wood Identification Using DART-TOFMS and the ForeST© Database: A Validation Study," *Forensic Science International: Animals and Environments* 2 (2022): 100045, https://doi.org/10.1016/j.fsiae.2022.100045.

83. X. Fan, B. Jiao, X. Zhou, W. Zhang, and Z. Ouyang, "Miniaturization of Mass Spectrometry Systems: An Overview of Recent Advancements and a Perspective on Future Directions," *Analytical Chemistry* 97 (2025): 9111–9125, https://doi.org/10.1021/acs.analchem.5c01223.

Supporting Information

Additional supporting information can be found online in the Supporting Information section.